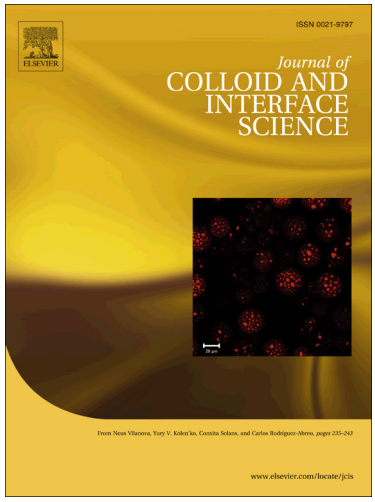

Self-assembly in dilute mixtures of non-ionic and anionic surfactants and rhamnolipd biosurfactants

J.R. Liley, J. Penfold, R.K. Thomas, I.M. Tucker, J.T. Petkov, P.S. Stevenson, I.M. Banat, R. Marchant, M. Rudden, A. Terry, I. Grillo

PII: S0021-9797(16)30838-4
DOI: http://dx.doi.org/10.1016/j.jcis.2016.10.071
Reference: YJCIS 21704

To appear in: *Journal of Colloid and Interface Science*

Received Date: 12 October 2016
Revised Date: 24 October 2016
Accepted Date: 25 October 2016

Please cite this article as: J.R. Liley, J. Penfold, R.K. Thomas, I.M. Tucker, J.T. Petkov, P.S. Stevenson, I.M. Banat, R. Marchant, M. Rudden, A. Terry, I. Grillo, Self-assembly in dilute mixtures of non-ionic and anionic surfactants and rhamnolipd biosurfactants, *Journal of Colloid and Interface Science* (2016), doi: http://dx.doi.org/10.1016/j.jcis.2016.10.071

Self-assembly in dilute mixtures of non-ionic and anionic surfactants and rhamnolipd biosurfactants

J.R. Liley[1†], J. Penfold[1,2], R.K. Thomas[1], I.M. Tucker[3], J. T. Petkov[3‡], P. S. Stevenson[3], I. M. Banat[4], R. Marchant[4], M. Rudden[4], A. Terry[2], I. Grillo[5]*

1. Physical and Theoretical Chemistry Laboratory, Oxford University, South Parks Road, Oxford, UK

2. ISIS, STFC, Rutherford Appleton Laboratory, Chilton, Didcot, Oxon, UK

3. Unilever Research and Development Laboratory Port Sunlight, Quarry Road East, Bebington, Wirral, UK

4. School of Bio-medical Sciences, University of Ulster, Coleraine, Northern Ireland, UK.

5. Insitut-Laue Langevin, 71 Avenue des martyrs, CS 20156, 38042, Grenoble, Cedex 09, France

* Corresponding Author: jeff.penfold@stfc.ac.uk

† Current Address: LGC, Queens Road, Teddington, Middlesex, TW11 0LY, UK

‡ Current Address: Lonza UK, GB-Blackley, Manchester, LANCS, M9 8ES

RECEIVED DATE (to be automatically inserted after your manuscript is accepted if required according to the journal that you are submitting your paper to)

ABSTRACT

The self-assembly of dilute aqueous solutions of a ternary surfactant mixture and rhamnolipid biosurfactant / surfactant mixtures has been studied by small angle neutron scattering. In the ternary surfactant mixture of octaethylene glycol monododecyl ether, $C_{12}E_8$, sodium dodecyl 6-benzene sulfonate, LAS, and sodium dioxyethylene monododecyl sulfate, SLES, small globular interacting micelles are observed over the entire composition and concentration range studied. The modelling of the scattering data strongly supports the assumption that the micelle compositions are close to the solution compositions. In the 5-component rhamnolipid / surfactant mixture of the mono-rhamnose, R1, di-rhamnose, R2, rhamnolipids with $C_{12}E_8$ / LAS / SLES, globular micelles are observed over much of the concentration and composition range studied. However, for solutions relatively rich in rhamnolipid and LAS, lamellar / micellar coexistence is observed. The transition from globular to more planar structures arises from a synergistic packing in the 5 component mixture. It is not observed in the individual components nor in the ternary $C_{12}E_8$ / LAS / SLES mixture at these relatively low concentrations. The results provide an insight into how synergistic packing effects can occur in the solution self-assembly of complex multi-component surfactant mixtures, and give rise to an unexpected evolution in the phase behaviour.

HIGHLIGHTS

- Self-assembly of ternary and 5-component surfactant mixtures studied
- In ternary mixtures, scattering data modelled as globular interacting micelles
- In ternary mixtures, variation in aggregation number implies micelle composition close to solution composition
- In 5-component mixture addition of rhamnolipid biosurfactants affects evolution in phase behaviour
- For rhamnolipid rich compositions transition from micelle to lamellar / micellar co-existence occurs
- Transition associated with synergistic packing effects

INTRODUCTION

A wide variety of different biosurfactants are produced by different bacteria. Their natural role has long been of some interest (1), but increasingly their use in biodegradable and biosustainable surfactant based products has become a focus of attention (2-6). One of the most commonly studied and exploited classes of biosurfactants are the glycolipids (7, 8), which are disaccharides that are acetylated by long chain fatty acids. The rhamnolipids are one of the most extensively studied and most promising biosurfactant (9). In addition to the advantages of bisosustainable and biodegradable products, the lower toxicity, higher tolerance to pH, temperature and salinity and their production from non-petrochemical based sources enhance their potential for many applications. Hence they have already been exploited in niche areas associated with enhanced oil recovery (4), bioremediation (6), in specialised healthcare and cosmetics applications (7), and in some aspects of detergency (10). More widespread incorporation into surfactant based products is limited by the need for improved yields and scale up, ease of purification, and the requirement for non-pathogenic bacterial sources (11, 12).

One of the more immediate and promising routes to the wider use of biosurfactants, and especially rhamnolipids, in a wider range of surfactant based products is their incorporation with surfactants from conventional sources. The adsorption and self-assembly of rhamnolipids has been addressed in a range of recent studies (13-24), but there is relatively little information on their behaviour with other surfactants (25-27). In contrast, in the field of conventional surfactants the study of surfactant mixing is a mature activity, and many of the basic phenomena associated with ideal and non-ideal mixing are well established experimentally and theoretically (28-33). More recently the application of new experimental methods, and particularly small angle neutron scattering, SANS, and neutron reflectivity, NR, to probe surfactant mixing in micelles and at interfaces has provided new insights (34, 35), and challenged some aspects of the current thermodynamic treatments of non-ideal mixing (35, 36).

NR has been used to study the adsorption of a range of relevant binary surfactant, some ternary surfactant (37), and some multi-component surfactant (38) mixtures at the air-water interface (34). The recent studies on the adsorption of the ternary mixture $C_{12}E_8$ / LAS / SLES (39) and the 5-component mixture of R1 / R2 / $C_{12}E_8$ / LAS / SLES (40) are of particular relevance to this study. SANS studies on multi-component mixed surfactant micelles are less common, but a

number of recent studies are particularly relevant (25, 26, 41-44). In the absence of electrolyte the LAS / non-ionic (43) and SLES / non-ionic (44) mixed micelles are globular and their aggregation numbers are consistent with a micelle composition close to the solution composition. This is observed in a range of ionic / non-ionic surfactant mixtures at concentrations >> critical micellar concentration, cmc (41-44). At lower surfactant concentrations, as the cmc is approached, the micelle composition evolves and becomes richer in the more surface active components (34, 41, 42); as predicted for non-ideal and ideal mixing by the pseudo-phase approximation (30). Hence in general at concentrations well above the cmc the mixed micelle structures reflect the structures of the pure component micelles. In the examples cited above, the preferred curvature of LAS, SLES, SDS and the non-ionic cosurfactants $C_{12}E_6$, $C_{12}E_8$ and $C_{12}E_{12}$ favour small globular structures at relatively low surfactant concentrations. LAS shows a slightly different trend at higher concentrations (≥100 mM) and has a greater tendency towards more planar structures (43, 45); and this has an impact on mixed micelle structures involving LAS. Hence in such cases, the competition between the relative preferred curvature in different surfactant components will determine the evolution in the micelle structure. This is observed more acutely in the rhamnolipid based systems (24, 25). R1 and R2 both form globular micelles at low surfactant concentrations ≤ 20 mM. R2, with the larger dirhamnose headgroup, remains globular up to relatively high surfactant concentrations. R1, with the smaller monorhamnose headgroup, has a lower preferred curvature and forms planar structures (lamellar or vesicular) at concentrations > 20 mM. In R1 / R2 mixtures the micelles remain globular at low surfactant concentrations, ≤ 20 mM; but a higher concentrations an evolution in the structure from globular to planar structures results from the competition between the preferred curvature associated with R1 and R2 (24). A similar tension is observed in R1 / LAS and R2 / LAS mixtures (25). R2 / LAS mixtures are predominantly globular, apart from LAS rich compositions at relatively high surfactant concentrations. R1 / LAS mixtures are however predominantly planar. In the R1 / R2 / LAS ternary mixture the evolution in the self-assembly is complex (25), and arises from the competition between the three different preferred curvatures.

These recent examples highlight the potential for a complex evolution in micelle structure in multi-component surfactant mixtures, and which are not necessarily easily predicted. In this paper we have used SANS to probe the micelle structure and the role of the relative preferred curvature on that structure in the biosurfactant / surfactant mixture of R1 / R2 / $C_{12}E_8$ / LAS /

SLES. The associated binary mixtures of $C_{12}E_8$, LAS and SLES and the ternary mixtures of $C_{12}E_8$, LAS and SLES in the absence of rhamnolipid, are also studied. The results provide an important insight into the evolution in the bulk structures, and have important consequences for the formulation of biosurfactant / surfactant mixtures.

EXPERIMENTAL DETAILS

(i) Small angle neutron scattering

In small angle scattering the pattern of the scattering intensity with wave vector transfer, Q (where Q is defined as $Q=4\pi/\lambda\sin(\theta)$, λ is the neutron wavelength, and 2θ is the scattering angle) from a micellar solution contains information about the micelle structure and inter-micellar interactions (46). For a solution of globular polydisperse interacting micelles the scattered intensity can be expressed in the 'decoupling approximation' as (46),

$$I(Q) = n\left[S(Q)\left|\langle F(Q)\rangle_Q\right|^2 + \left\langle \left|F(Q)\right|^2 \right\rangle_Q - \left|\langle F(Q)\rangle_Q\right|^2 \right] \quad (1)$$

where the average $\langle\ \rangle_Q$ denotes averaging over micelle sizes and orientations, n is the micelle number density, F(Q) the micelle form factor and S(Q) the inter-micellar structure factor. S(Q) is modelled using the rescaled mean spherical approximation, RMSA, calculated for a repulsive screened coulombic potential (47, 48). As such, S(Q) is defined by the micelle surface charge, z, the micelle number density, n, the micelle diameter, and the Debye-Hückel inverse screening length, κ^{-1} (47).

The SANS measurements were made on three different small angle scattering diffractometers, LOQ (49) and SANS2D (50) at the ISIS neutron source, and D33 (51) at the Institute Laue Langevin. On LOQ and SANS2D the measurements were made using the white beam time of flight method. On LOQ a neutron wavelength range of 2-10 Å and a sample to detector distance of 4.15 m was used to cover a Q range of 0.008 to 0.25 $Å^{-1}$. On SANS2D a Q range of 0.01 to 0.35 $Å^{-1}$ was covered using neutron wavelengths of 2-12 Å and a sample to detector distance of 2.42 m. On D33 the measurements were made in monochromatic mode with a neutron wavelength of 4.6 Å ($\Delta\lambda/\lambda$ ~ 10%) and two detector arrays at 2 and 12 m from the sample position to cover a Q range of 0.004 to 0.3 $Å^{-1}$. In all cases an 8 mm diameter beam was used, and the measurement times were ~ 10 to 20 minutes per sample for 1 mm path length samples. The scattering from the cell and solvent were subtracted from the data. The data were

normalised to the detector response and spectral distribution of the incident beam to establish the scattered intensity, I(Q), as an absolute scattering cross-section using standard procedures (52, 53).

(ii) Materials and Measurements made

All the surfactant solution were prepared using the hydrogeneous form of the surfactants with D_2O as the solvent. All the solutions were measured at 25 °C and in 10^{-6} M NaOH to provide a nominal pH of 8. The solutions were contained in 1 mm path length Hellma quartz spectrophotometer cells. All cells and associated glassware used to prepare the solutions were cleaned in dilute (2%) Decon90 solution and rinsed in MilliQ Ultrapure water, rinsed in acetone and dried in an air flow. The $C_{12}E_8$ was obtained from Nikkol and used as supplied. The LAS was synthesised and purified as described elsewhere (43). The SLES was synthesised and purified by recrystallization from ethanol / acetone mixtures as described by Xu et al (54). The rhamnolipids L-rhamnosyl-L-rhamnosyl-β-hydroxydecanol-β-hydroxydecanoate, R1, and L-rhamnosyl-β-hydroxydecanol-β-hydroxydecanoate, R2, were obtained from Jeneil Biosurfactant Co and separated into pure R1 and R2 components as described elsewhere (24), and the structure of R1 and R2 are shown in figure 1.

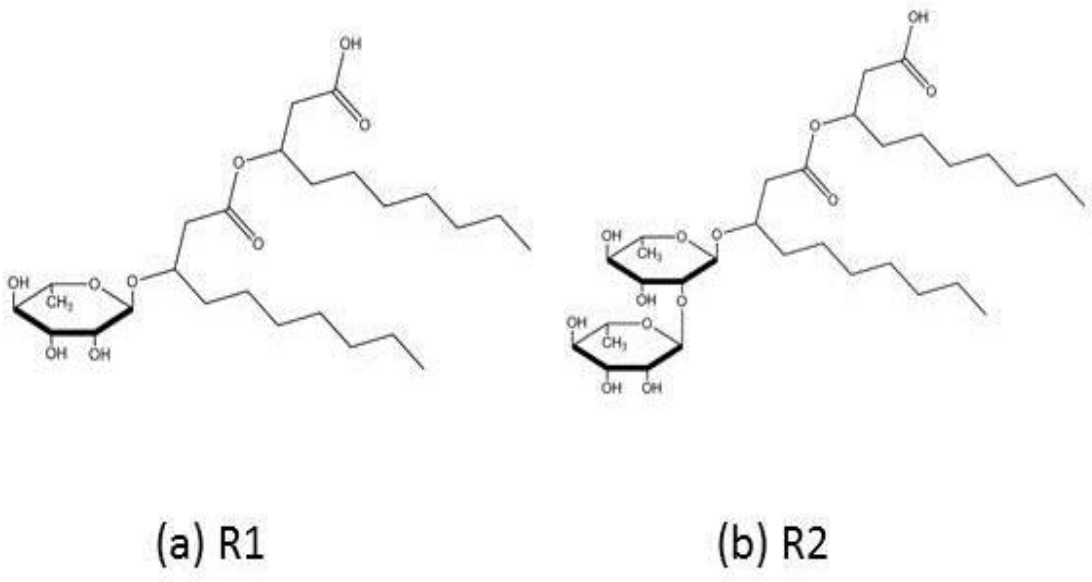

***Figure 1**. Structure of the rhamnolipids R1, and R2*

The binary and ternary mixtures of $C_{12}E_8$, LAS and SLES were measured at surfactant concentrations of 10, 25 and 50 mM and over a wide range of compositions. The 5-component R1 / R2 / $C_{12}E_8$ / LAS / SLES mixtures were also measured at 10, 25 and 50 mM. These measurements were made for a range of $C_{12}E_8$ / LAS / SLES compositions in which 20 or 30 mole% of the ternary surfactant mixture is replaced by an R1 / R2 mixture. The measurements were made for both 1:1 and 2:1 R1 / R2 mixtures. The measurements of the mixtures of $C_{12}E_8$, LAS and SLES and the 5-component mixtures were made on LOQ and SANS2D, with the measurements at the lower surfactant concentrations predominantly on SANS2D. D33 was used for measurements of the 5-component mixtures which were rich in LAS.

RESULTS and DISCUSSION

For the binary and ternary surfactant mixtures of $C_{12}E_8$, LAS and SLES and for some of the 5-component R1 / R2 / $C_{12}E_8$ / LAS / SLES mixtures the form of the self-assembly is identified from the scattering pattern. The data consists of regions of globular interacting micelles or a mixed micellar / lamellar (vesicular) phase. The data for the globular interacting micelles are analysed quantitatively using the standard 'core and shell' model for globular micelles (46) using equation 1. The micelle form factor, F(Q), is given by (46),

$$F(Q) = V_1(\rho_1 - \rho_2)F_0(Qr_1) + V_2(\rho_2 - \rho_s)F_0(Qr_2) \qquad (2)$$

$$F_0(Qr_i) = 3[\sin(Qr_i) - Qr_i\cos(Qr_i)]/(Qr_i)^3 \qquad (3)$$

and r_1, r_2 are the core and shell radii, $V_i = 4\pi r_i^3/3$, ρ_1, ρ_2 and ρ_s are the scattering length densities of the micelle core and shell, and of the solvent ($\rho_i = N_i b_i$ and N_i, b_i are the number density and the scattering length of the i^{th} component). Molecular and packing constraints are used to define and constrain the core and shell model. The inner core has a radius r_1 which contains the surfactant alkyl chains in a volume constrained to have a maximum radius equal to the fully extended alkyl chain length, l_c, of the surfactant. A model parameter, ext, allows some variation in the packing constraint, and is generally in the region 1.0 to 1.3, For micelle aggregation numbers, ν, greater than can be accommodated in a sphere of radius l_c a prolate ellipsoid shape is assumed, with core dimensions of r_1 and r_1. ee, where ee is the ellipticity ratio. For spherical or ellipsoidal shapes the outer shell radius, r_2, is constrained to contain the headgroups and associated hydration. The surfactant mixing is taken into account by using a

composition weighted average of the parameters associated with each surfactant and assuming that the micelle composition reflects the solution composition. S(Q) is calculated using the RMSA, as described earlier. From the known molecular volumes and dimensions and associated scattering lengths, the scattering is calculated on an absolute scale, compared with the data and evaluated by least squares. An acceptable model requires that the functional form of the scattering is reproduced and the absolute scattering is predicted to within ±20%. The data for the mixed micellar / lamellar (vesicular) phase are not analysed quantitatively.

(i) Binary Mixtures

SANS measurements were made for the binary mixtures of $C_{12}E_8$ / SLES, $C_{12}E_8$ / LAS and LAS / SLES at surfactant concentrations of 10, 25 and 50 mM and over a range of surfactant compositions. The data presented in figure 2 are for the $C_{12}E_8$ / SLES mixture. In figure 2a the data are for 0.5 / 0.5 mole ratio of $C_{12}E_8$ / SLES at surfactant concentrations of 10, 25, and 50 mM. In figure 2b the data are from a 25 mM solution of $C_{12}E_8$ / SLES at solution compositions of 0.75 / 0.25, 0.5 / 0.5, 0.25 / 0.75, and 0.1 / 0.9 mole ratios.

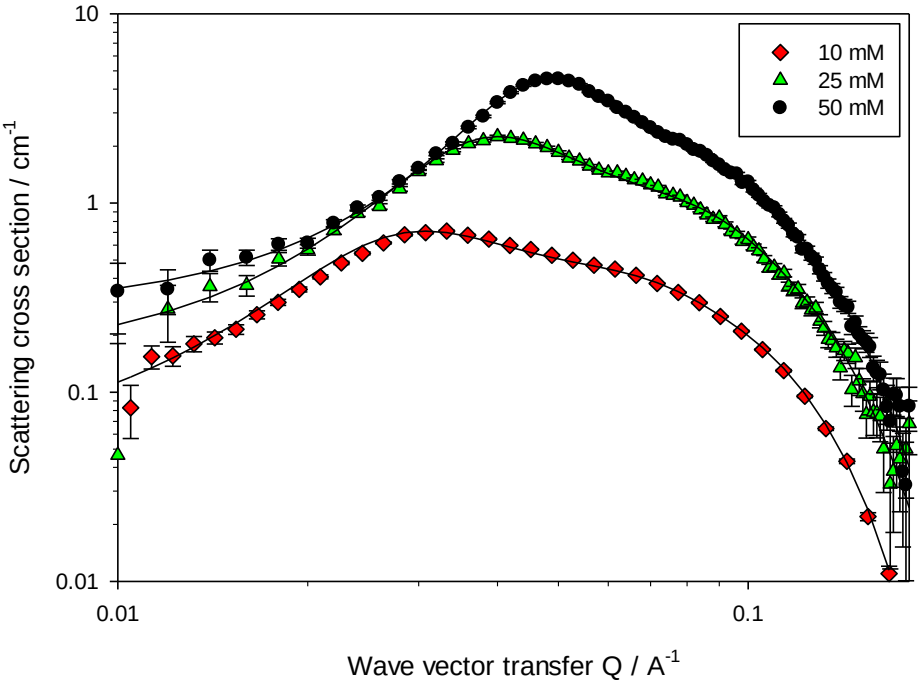

(a)

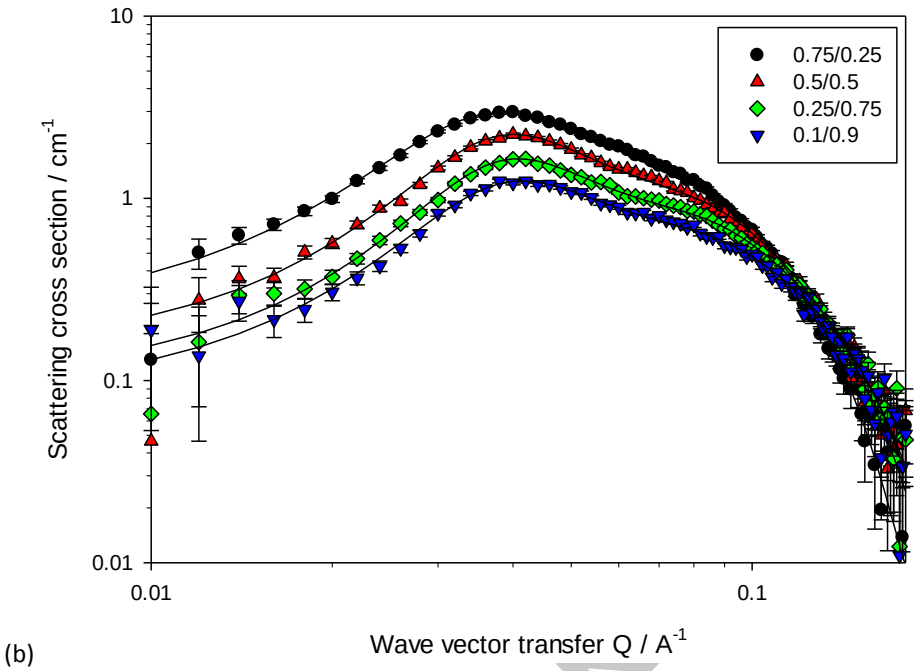

Figure 2. *SANS data for (a) 0.5/0.5 $C_{12}E_8$ / SLES at 10mM, 25mM and 50mM, and (b) 25 mM $C_{12}E_8$ / SLES at compositions 0.75/0.25, 0.5/0.5, 0.25/0.75 and 0.1/0.9, at 25mM. See legend for details. The solid lines are model calculations as described in the text and for the key model parameters summarised in table 1, and in table S1 in the Supporting Information.*

The data in figure 2 are consistent with relatively small globular interacting micelles, and are well described by the core and shell model of interacting micelles (46). In figure 2a the interaction peaks in the data shifts to lower Q values as the micelle number density increases, and the scattering intensity increases as the total surfactant concentration increases. In figure 2b the variation in the scattering pattern with composition at a fixed surfactant concentration reflects the change in the aggregation number and form factor from SLES to $C_{12}E_8$ rich compositions.

Table 1. *Key model parameters from core and shell model analysis of SANS data for $C_{12}E_8$ / SLES mixed surfactants.*

Surfactant concentration (mM)	**Solution composition ($C_{12}E_8$/SLES mole ratio)**		**ν (±5)**	**z (±1)**	**δ (±0.02)**	**r1 (±1 Å)**	**r2 (± 1Å)**	**ext (±0.05)**	**ee (±0.02)**
	$C_{12}E_8$	**SLES**							
10	0.5	0.5	82	16	0.20	18	23	1.10	1.42
25	0.1	0.9	93	17	0.18	18	25	1.10	1.12
25	0.25	0.75	92	19	0.21	18	23	1.10	1.16
25	0.5	0.5	96	19	0.20	18	24	1.10	1.21
25	0.75	0.25	109	15	0.14	18	25	1.10	1.37
50	0.5	0.5	100	22	0.22	18	24	1.10	1.26

At a fixed composition (see figure 2a) as the surfactant concentration increases there is a modest increase in the micelle aggregation number. At a fixed concentration, as the solution composition varies from SLES to $C_{12}E_8$ rich the aggregation number varies more significantly, but dependent upon the surfactant concentration. At a surfactant concentration of 10 mM it increases from 67 to 101. At surfactant concentrations of 25 and 50 mM the increase is more modest, and is from ~90 to 100. These changes reflect the aggregation number of the pure component micelles. SLES has an aggregation number ~75 at 10 mM and ~90 at 25 mM (54). The aggregation number for $C_{12}E_8$ is ~110 and varies little with surfactant concentration in the concentration range measured here (43). The variation in the degree of micelle ionisation, δ, (where δ=z/ν) reflects the change from $C_{12}E_8$ to SLES rich micelles. For the $C_{12}E_8$ rich compositions the degree of ionisation is systematically lower, similar to the trend reported for SDS / $C_{12}E_8$ micelles (42). However, the degree of ionisation for the SLES rich micelles is also relatively low compared to other ionic surfactant micelles. δ is ~ 0.2, whereas ionic micelles in general have a δ ~ 0.3 to 0.35 (46). This was discussed at length by Xu et al (54, 55), where it was observed that SLES is only relatively weakly dissociated.

Broadly similar data are observed for $C_{12}E_8$ / LAS and LAS / SLES surfactant mixtures, and the data are summarised in tables S2 and S3 and figures S1 and S2 in the Supporting Information. For both the $C_{12}E_8$ / LAS and LAS / SLES mixtures the SANS data are again consistent with globular interacting micelles. The aggregation number for the $C_{12}E_8$ / LAS

mixture varies with solution composition and concentration from ~70 to ~110; whereas for the LAS / SLES mixture it varies from ~ 45 to ~90. As with the $C_{12}E_8$ / SLES mixture these variations reflect the aggregation of the pure component micelles. For LAS the aggregation number is ~ 30 at 109 mM, ~40 at 25 mM and ~47 at 50 mM (43). The greater variation in the aggregation number for the LAS containing mixtures reflect the much lower LAS aggregation number compared to that for SLES or $C_{12}E_8$. The degree of ionisation of the LAS / SLES and LAS / $C_{12}E_8$ mixtures is low compared to other charged micelles, and is $\leq$ 0.2. It is also especially low for $C_{12}E_8$ and SLES rich micelles, as was also observed for the $C_{12}E_8$ / SLES micelles earlier. In all three binary mixtures, $C_{12}E_8$ / SLES, LAS / $C_{12}E_8$ and LAS / SLES the quality of the model fits, in terms of the form of the scattering and the absolute scale of the scattering, are such that the assumption that the micelle composition reflects the solution composition is justified. Hence the variation in the micelle aggregation is a weighted average of the aggregation numbers associated with the pure micellar components

Ternary Mixtures

SANS measurements were made for the ternary mixture of $C_{12}E_8$ / LAS / SLES at surfactant concentrations of 10, 25 and 50 mM, and over a range of compositions. The compositions over which the measurements were made are summarised in the ternary diagram shown in figure 3.

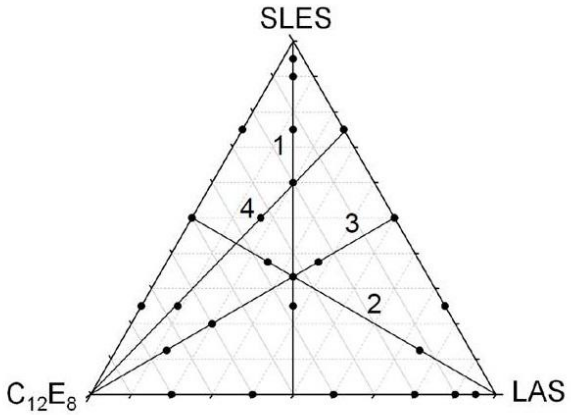

Figure 3. *Ternary $C_{12}E_8$ / LAS / SLES diagram, showing the points at which SANS measurements were made; where line 1 represents equal $C_{12}E_8$ and LAS mole fractions, line 2 equal $C_{12}E_8$ and SLES mole fractions, line 3 equal SLES and LAS mole fractions, line 4 differing $C_{12}E_8$, LAS and SLES mole fractions, and the edges of the triangle the binary mixtures.*

All the SANS data for the ternary mixtures are consistent with the scattering from interacting globular micelles, and hence broadly similar to the data shown in figure 2. The SANS data for a 0.33 / 0.33 / 0.33 mole ratio mixture of $C_{12}E_8$ / LAS / SLES at surfactant concentrations of 10, 25 and 50 mM, and the variation in the SANS data with composition at a surfactant concentration of 50 mM are shown in figures S4a and S4b in the Supporting Information. A full summary of the key model parameters for the core and shell model fits to the ternary data can be found in table S4 in the Supporting Information.

The key model parameters corresponding to the data shown in figures S3 a and b are also summarised here in tables 2 and 3.

Table 2. *Key model parameters for core and shell model fit to SANS data for 0.33 / 0.33 / 0.33 mole ratio mixture of $C_{12}E_8$ / LAS / SLES at surfactant concentrations of 10, 25 and 50 mM.*

Surfactant concentration (mM)	**ν (±5)**	**z (±1)**	**δ (±0.02)**	**r1 (±1 Å)**	**r2 (± 1Å)**	**ext (±0.05)**	**ee (±0.02)**
10	65	14	0.22	17	21	1.12	1.44
25	83	16	0.19	19	26	1.45	1.00
50	86	18	0.21	18	23	1.17	1.31

Table 3. *Key model parameters for core and shell model fit to SANS data for $C_{12}E_8$ / LAS / SLES mixture with different compositions at a surfactant concentration 50 mM.*

Solution composition ($C_{12}E_8$/LAS /SLES mole ratio)			**ν (±5)**	**z (±1)**	**δ (±0.02)**	**r1 (±1 Å)**	**r2 (± 1Å)**	**ext (±0.05)**	**ee (±0.02)**
$C_{12}E_8$	**LAS**	**SLES**							
0.25	0.375	0.375	85	19	0.22	20	24	1.28	1.01
0.33	0.33	0.33	86	18	0.21	18	23	1.17	1.31
0.75	0.125	0.125	107	15	0.14	18	25	1.13	1.42

At the fixed solution composition of 0.33 / 0.33 / 0.33 $C_{12}E_8$ / LAS / SLES (see table 2) the aggregation number increases with increasing surfactant concentration, from ~65 to ~90 at the highest surfactant concentration, and the degree of ionisation is relatively constant. At the fixed surfactant concentration of 50 mM and variable $C_{12}E_8$ / LAS / SLES composition (see table 3)

the aggregation number increases as the solution composition becomes richer in the non-ionic $C_{12}E_8$ and the degree of ionisation decreases significantly.

The three lines or cuts through the ternary diagram shown in figure 3 are lines in which the composition of one of the components, SLES (line 1), LAS (line 2) and $C_{12}E_8$ (line 3) varies and the other two components have equal but varying compositions. Along the lines of increasing SLES or $C_{12}E_8$ composition the aggregation number increases, and for the line of increasing LAS composition it decreases; as shown in the data in table S4. As observed for the binary mixtures the model fits are consistent with the assumption that the micelle composition reflects the solution composition, and the micelle aggregation numbers are again a weighted average of the pure components.

Hence, in general, in the binary and ternary mixtures the variation in the micelle aggregation number reflects the values of the pure component micelles of $C_{12}E_8$, LAS and SLES. This is illustrated more completely in figure 4, where the variation in aggregation number for the ternary mixtures as a function of solution composition over the entire composition range and concentrations measured are shown as colour contour ternary diagrams.

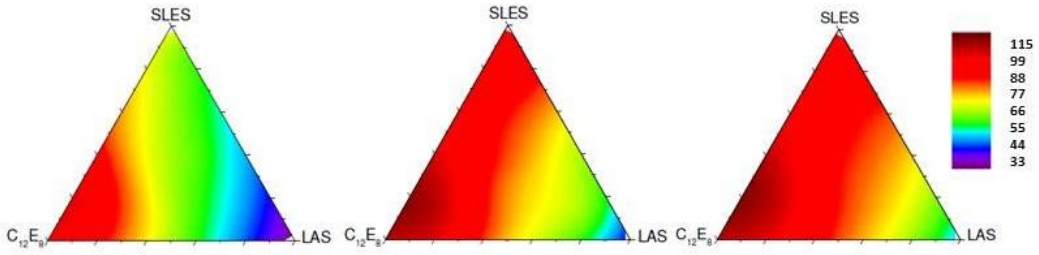

Figure 4: *Variation in aggregation number with solution composition, at (a) 10 mM, (b) 25 mM and (c) 50 mM. The legend indicates the colour scale which ranges from 33 (purple) to 115 (red).*

(ii) 5–component R1 / R2 / $C_{12}E_8$ / LAS / SLES mixture

SANS measurements were made for the 5-component R1 / R2 / $C_{12}E_8$ / LAS / SLES mixture at surfactant concentrations of 10, 25 and 50 mM. The measurements were made for variable $C_{12}E_8$ / LAS / SLES compositions, over a similar composition range to those used for the ternary mixture earlier. In the 5-component mixtures a fraction of the $C_{12}E_8$ / LAS / SLES ternary mixture is replaced by a fixed mole fraction of R1 / R2, 20 and 30 mole %, and for two different R1 / R2 mole ratios, 1:1 and 2:1.

Over much of the solution composition range, but especially regions which are relatively rich in $C_{12}E_8$ or SLES, the resultant scattering is similar to that observed for the binary and ternary mixtures, and is consistent with interacting globular micelles. The aggregation number and other key model parameters are summarised in table S5 in the Supporting Information for some of the data measured. In these regions the addition of R1 / R2 has relatively little impact upon the form and size of the micelles. This is illustrated in table 4 for a selected region of data at a surfactant concentration of 50 mM. The key model parameters for four different $C_{12}E_8$ / LAS / SLES compositions are compared with those in which 30 mole % of the $C_{12}E_8$ / LAS / SLES mixture is replaced by a 1:1 mole ratio mixture of R1 / R2.

Table 4. *Key model parameters from core and shell model analysis of SANS data for 50 mM $C_{12}E_8$ / LAS / SLES at four different solution compositions (a) ternary $C_{12}E_8$ / LAS / SLES mixture, (b) 30 mole % of ternary mixture replaced by 1:1 mole ratio R1 / R2 mixture*

(a) Ternary mixture

Solution composition ($C_{12}E_8$/LAS /SLES mole ratio)			**ν (±5)**	**z (±1)**	**δ (±0.02)**	**r1 (±1 Å)**	**r2 (± 1Å)**	**ext (±0.05)**	**ee (±0.02)**
$C_{12}E_8$	**LAS**	**SLES**							
0.33	0.33	0.33	86	18	0.21	18	23	1.17	1.31
0.375	0.375	0.25	86	17	0.20	18	23	1.18	1.31
0.375	0.25	0.325	90	19	0.21	19	25	1.34	1.00
0.25	0.375	0.375	85	19	0.22	19	20	1.28	1.01

(b) 5-component mixture

Solution composition ($C_{12}E_8$/LAS /SLES mole ratio)*			**ν (±5)**	**z (±1)**	**δ (±0.02)**	**r1 (±1 Å)**	**r2 (± 1Å)**	**ext (±0.05)**	**ee (±0.02)**
$C_{12}E_8$	**LAS**	**SLES**							
0.23	0.23	0.23	80	13	0.16	17	21	1.13	1.70
0.26	0.26	0.18	81	13	0.16	17	21	1.12	1.82
0.26	0.18	0.26	82	13	0.16	17	22	1.14	1.58
0.18	0.26	0.26	78	13	0.17	17	21	1.12	1.74

* mole fraction of total solution composition: equivalent to mole ratios in table 4a.

From table 4 and table S5 in the Supporting Information the addition of the R1 / R2 mixture in the micellar region of the ternary $C_{12}E_8$ / LAS / SLES mixture has relatively little impact on the micelle aggregation number. However, the addition of the rhamnolipids results in a systematic decrease in the degree of micelle ionisation. This is consistent with the previous observations (24, 25) that R1 and R2 are only weakly ionic. Although the mean aggregation numbers are not greatly affected, the geometrical parameters, r_1, r_2 and ee the ellipticity ratio are different. This is due to changes in the molecular constraints in the model arising from the inclusion of R1 and R2; and this will be discussed in more detail later in the discussion

However, for solutions relatively rich in LAS, the addition of R1 / R2 results in a pronounced change in the solution microstructure. Replacing part of the $C_{12}E_8$ / LAS / SLES mixture with R1 / R2 results in a transition from globular micelles to micellar / lamellar coexistence for LAS rich compositions. This is illustrated in figure 5, where the SANS data for 25 and 50 mM 0.125 / 0.75 / 0.125 mole ratio $C_{12}E_8$ / LAS / SLES is shown, in the absence and presence of 30 mole% replacement by a 1:1 mole ratio mixture of R1 / R2.

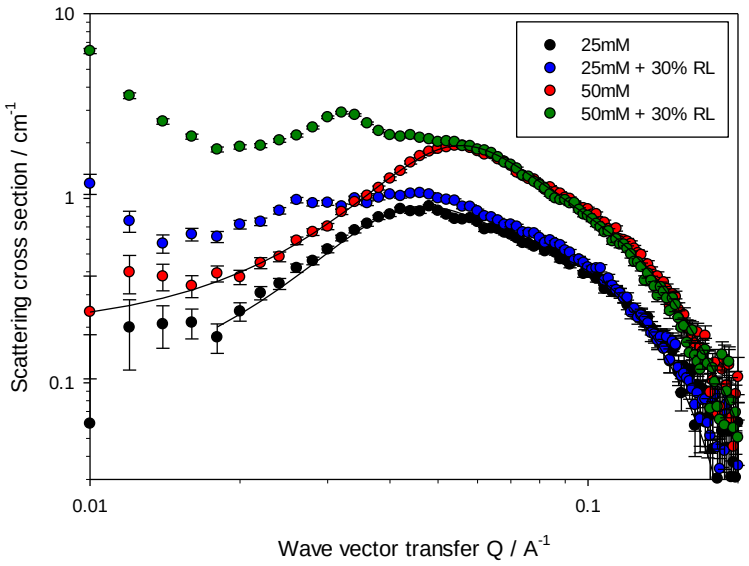

Figure 5. *SANS data for 0.125 / 0.75 / 0.125 mole ratio $C_{12}E_8$ / LAS / SLES at 25 and 50 mM, in the absence and presence of 30 mole% replacement by a 1:1 mole ratio mixture of R1 / R2. See legend for details. The solid lines are model fits as described in the text.*

In the absence of the rhamnolipid the scattering from the ternary $C_{12}E_8$ / LAS / SLES mixture is consistent with globular interacting micelles, as previously presented and discussed. At both surfactant concentrations the addition of the R1 / R2 mixture results in a marked change in the

form of the scattering. The scattering data now indicate the onset of the formation of lamellar (vesicle) structures, and the scattering is consistent with micellar / lamellar coexistance. This is not observed in the binary or ternary mixtures in the absence of the rhamnolipids, nor in the pure component micelles in this concentration range. The addition of the rhamnolipids to the LAS rich compositions of the $C_{12}E_8$ / LAS / SLES ternary mixture results in a synergistic impact upon the packing and relative preferred curvature of the self-assembly to promote the transition towards more planar structures.

In light of this further SANS measurements were made in the LAS rich region of the ternary $C_{12}E_8$ / LAS / SLES phase diagram, see figure 6, in order to explore in more detail the role of the ternary composition, the R1 / R2 mole ratio, and the rhamnolipid / ternary surfactant mole ratio.

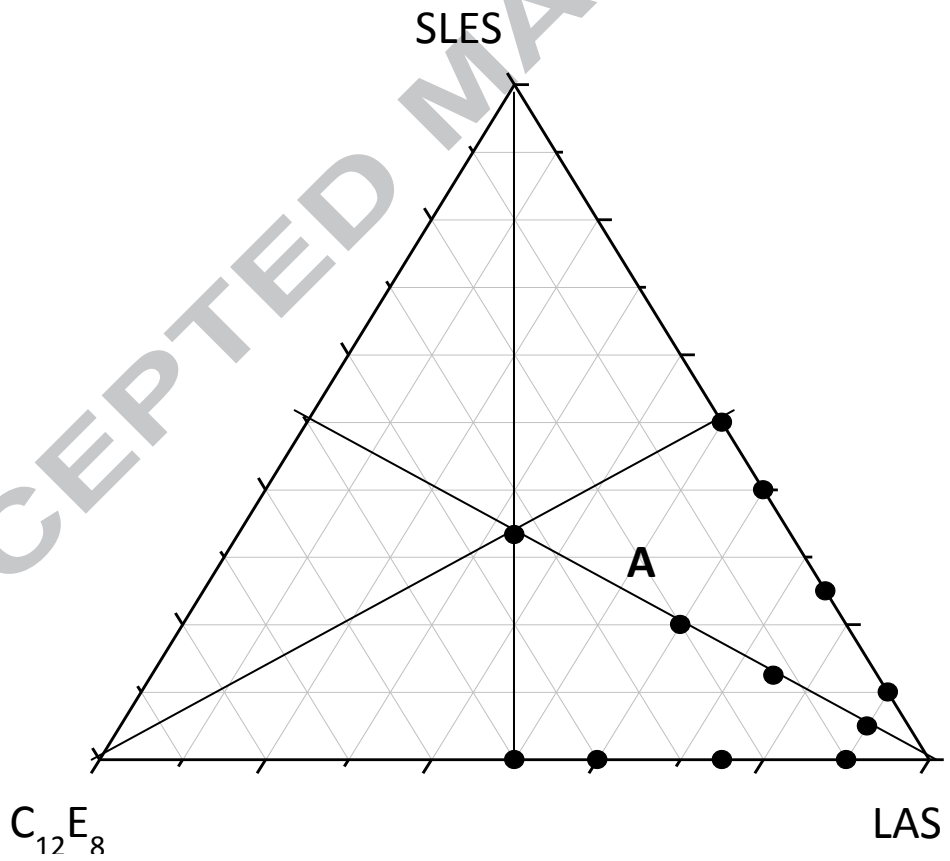

Figure 6. *Ternary diagram for $C_{12}E_8$ / LAS / SLES, showing compositions used for more detailed evaluation of the lamellar / micellar coexistence region.*

The impact of the changing LAS compositions is shown in figure 7; where the variation in the SANS data for 50 mM R1 / R2 / $C_{12}E_8$ / LAS / SLES is shown for a 30 / 70 rhamnolipid / surfactant mixture with an R1 / R2 mole ratio of 1:1. The data are taken along a line (marked as A) in figure 5, for LAS compositions of 0.23, 0.42, 0.53 and 0.63, with equal mole fractions of the remaining components.

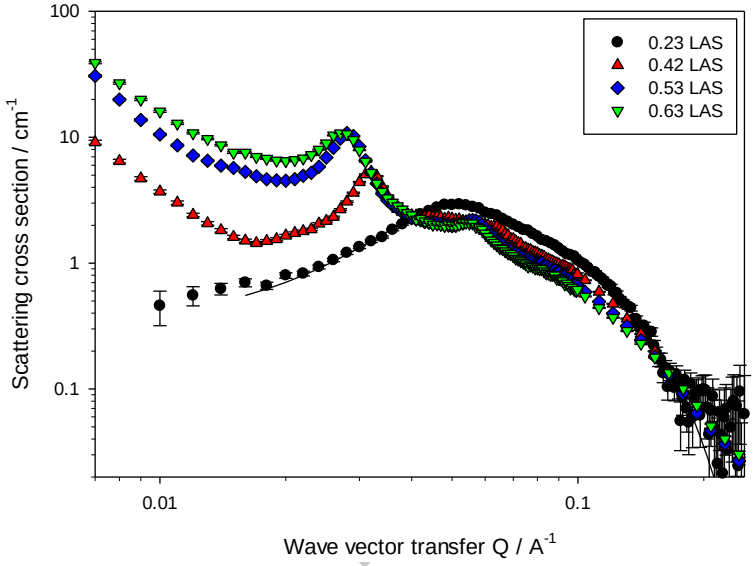

Figure 7. *SANS data for 50 mM R1/ R2 / $C_{12}E_8$ / LAS / SLES with 30 / 70 mole ratio R / C (rhamnolipid / conventional surfactant ratio), and R1 / R2 1:1 mole ratio. See legend for details. The R1, R2 mole ratios are 0.15, 0.15, and the $C_{12}E_8$ and SLES mole fractions are 0.24, 0.14, 0.08, and 0.035 respectively. The solid line for the micellar scattering is a model calculation as described in the main text.*

At the lowest LAS mole fraction, 0.23, the scattering is consistent with small globular interacting micelles. Between the LAS mole fractions of 0.23 and 0.42 the form of the scattering changes, as illustrated in figure 7. The increase in the scattering at low Q values and the appearance of first and second order Bragg peaks are indicative of the onset of a transition from micelles to more planar structures, lamellar or vesicular. The scattering then has components of both the micellar contribution at high Q and the lamellar component which is more visible at low Q, and is then consistent with micellar / lamellar (L_1 / L_α) coexistence. As the LAS mole fraction increases to 0.53 and 0.63 the lamellar component of the scattering increases and the micellar component decreases; such that at the higher LAS mole fractions the coexistence is more dominated by the lamellar structures, and is then L_α / L_1. The assignment

of L_1 / L_α or L_α / L_1 is purely qualitatively based on the relative contribution of the two scattering components.

Given that R1 like LAS has a greater tendency towards planar structures (24, 25) the rhamnolipid /surfactant and R1 / R2 mole ratios should have an impact upon the transition from micellar to planar structures. The effect of the rhamnolipid / surfactant ratio is illustrated in figure 8, for the R1 / R2 mole ratio of 2:1, a $C_{12}E_8$ / LAS / SLES composition of 0.125 / 0.75 / 0.125 mole ratio, and at rhamnolipid / surfactant mole ratios of 20 /80 and 30 /70, and at surfactant concentrations of 10, 25 and 50 mM.

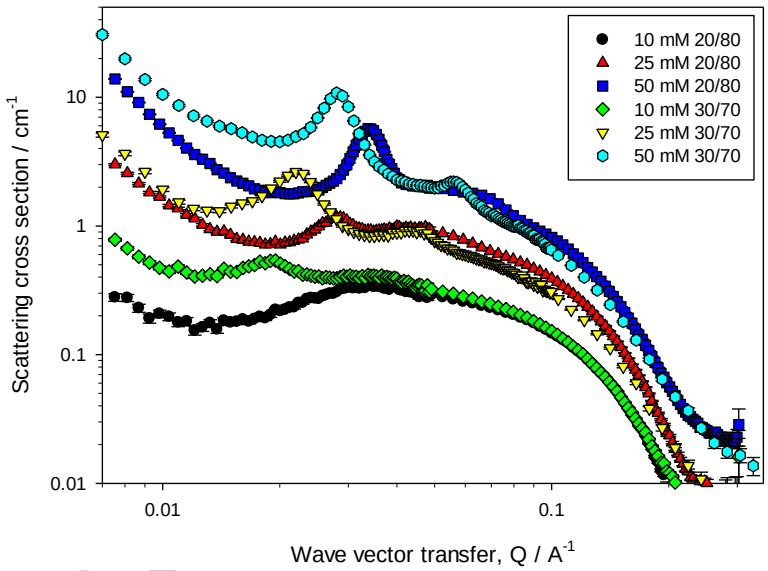

Figure 8. *SANS data for R1 / R2 / $C_{12}E_8$ / LAS / SLES at 20 / 80 and 30 / 70 rhamnolipd / surfactant, at a fixed R1 / R2 ratio of 2:1, at an equivalent $C_{12}E_8$ / LAS / SLES solution composition of 0.125 / 0.75 / 0.125, at 10, 25 and 50 mM, see legend for details.*

As the mole fraction of rhamnolipid increases from 20 to 30 mole % the lamellar component to the scattering increases significantly. As was shown also in figure 3 the tendency towards more planar structures increases with increasing surfactant concentration. This was observed for both LAS and R1 (24, 25, 43).

A similar trend is observed at a fixed rhamnolipid / surfactant ratio and composition of the $C_{12}E_8$, LAS and SLES components with increasing fraction of R1 compared to R2. This is illustrated in figure S4 in the Supporting Information. The data in figure S4 shows the SANS profiles for R1 / R2 / $C_{12}E_8$ / LAS / SLES at 25 and 50 mM for a 30 / 70 mole ratio rhamnolipid / surfactant mixture and an equivalent ternary $C_{12}E_8$ / LAS / SLES mixture with a mole ratio of 0.0 / 0.75 / 0.25, for two different R1 / R2 mole ratios of 1:1 and 2:1. At the

solution concentration of 25 mM the scattering is in the form of globular micelles, whereas at 50 mM it corresponds to L_1 / L_α coexistance. However the change in the R1 / R2 composition to a composition richer in R1, 2:1, results in a significant increase in the lamellar component at a surfactant concentration of 50 mM, and the appearance of a lamellar component at 25 mM. At both concetrations, for the R1 / R2 mole ratio of 2:1, the scattering is consistent with L_α / L_1, lamellar/ micellar, coexistance.

From the range of data obtained in the LAS rich region of the $C_{12}E_8$ / LAS / SLES ternary diagram, approximate phase diagrams have been determined. These show the effect of changing the rhamnolipid / surfactant mole ratio and the R1 / R2 mole ratio on the formation of lamellar stuctures in the 5-component R1 / R2 / $C_{12}E_8$ / LAS / SLES mixture; and are illustrated in figures 9 a and b.

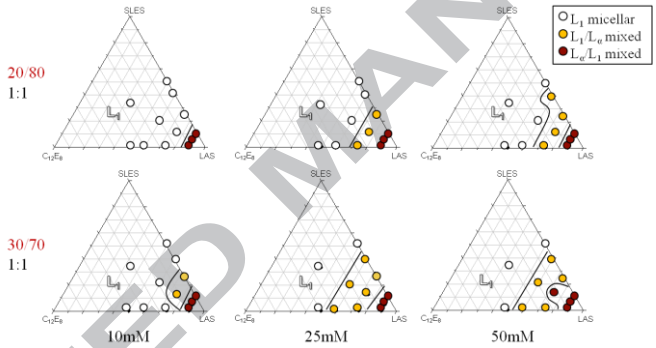

(a)

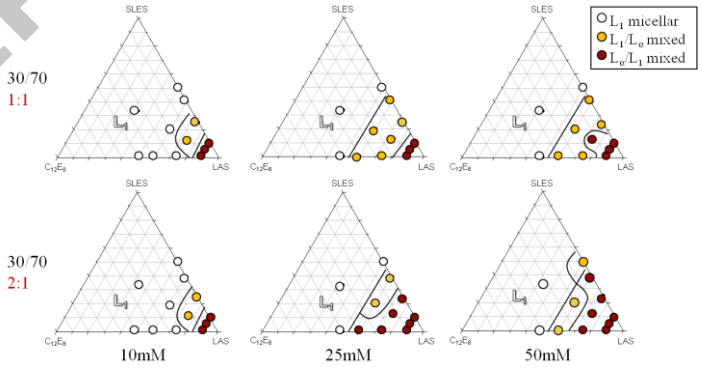

(b)

Figure 9. *Approximate qualitative phase diagrams for R1 / R2 / $C_{12}E_8$ / LAS / SLES surfactant mixtures, derived from SANS data, at 10, 25 and 50 mM, (a) variation in rhamnolipid / surfactant mole ratio, (b) variation in R1 / R2 mole ratio.*

The phase diagrams illustrate the main features and parameters associated with the transition from micellar to lamellar structures; where L_1 indicates micellar, L_1 / L_α, micellar / lamellar coexistance where the micellar component is dominant, and, L_α / L_1, lamellar / micellar coexistance where the lamellar component is dominant. The main features are, (i) the transition from micellar to lamellar occurs for the LAS rich region of the ternary $C_{12}E_8$ / LAS / SLES mixture, (ii) the transition is more pronounced as the amount of rhamnolipid increases and is only present when rhamnolipid is incorporated, (iii) the transition is more pronounced when the R1 / R2 ratio is richer in R1, and (iv) the tendency towards lamellar structures increases with increasing surfactant concentration.

(iii) Discussion

The scattering from the binary and ternary mixtures of $C_{12}E_8$ / LAS / SLES is consistent with globular interacting micelles, and the data are well described by the core + shell model of interacting micelles presented earlier. The consistency of the modelling supports the assumption that the micelle composition reflects the solution composition. This is as expected (29-31, 41-43) at concentrations well in excess of the mixed cmc. The variation in the micelle aggregation number then reflects the aggregation number of the pure components micelles of $C_{12}E_8$ (42, 43), LAS (43) and SLES (44, 54), and is a composition weighted average of the pure components.

Typically LAS has a micelle packing parameter, pp, ~ 0.56, (where the Israelachvili, Mitchell and Ninham packing parameter, pp, based on geometrical packing arguments and an effective criterion for predicting micelle morphology, pp=v/Al, v is the alkyl chain molecular volume, l is the extended alkyl chain length and A is the area / molecule, such that micelles are spherical for pp< 1/3, elongated for 1/3<pp>1/2 and planar for pp>1/2 (56)). Although LAS micelles are globular at low concentrations (43, 57), at higher there is a tendency towards planar structures (43, 45), consistent with the pp~ 0.6. However at the concentrations studied here, up to 50 mM, only globular micelles are observed. $C_{12}E_8$, due to its relatively large ethoxylated headgroup, has a pp ~ 0.32; and this is consistent with globular micelles, at the transition from spherical to elongated structures (42, 43). SLES (44, 45) has a pp~ 0.25, and is in the form of globular micelles up to relatively high concentrations. The variation in the micellar geometrical parameters, as defined by the core and shell radii, r_1 and r_2, and the ellipticity, ee, reflect the molecular constraints associated with the pure components. r_1 is largest for the $C_{12}E_8$ and SLES rich compositions as the fully extended C_{12} alkyl chain length is ~ 17 Å, compared to ~13 Å for

the di-C_6 chains of LAS (the values for LAS includes the phenyl ring). r_2 is largest for the $C_{12}E_8$ rich compositions, and this reflects the larger headgroup volume compared to SLES or LAS. The charge on the micelle, as quantified by the degree of ionisation, δ, is relatively low compared to ionic surfactant micelles. It varies with micelle composition, as expected for ionic / nonionic mixed surfactant micelles (41-43), and is lower for the nonionic rich micelle compositions. For ionic micelles, δ is typically ~ 0.3 to 0.35 (46, 58). δ has the highest value in the data presented here for LAS rich compositions, but is generally ≤ 0.2. It is especially low for $C_{12}E_8$ rich compositions, as expected, but for most of the data is generally lower than that reported in other mixed systems, for example, $C_{12}E_8$ / SDS (42). This is because the the degree of ionisation is also anomalously low for SLES (54, 55); where it is typically ≤ 0.15. SLES is only weakly dissociated (54, 55), and this was previously attributed to the stronger counterion binding arising from a decrease in the dielectric constant associated with the ethoxylated environment of the headgroup.

For the 5-component mixture of R1 / R2 / $C_{12}E_8$ / LAS / SLES, over much of the composition range explored and at the relatively low surfactant concentrations used, ≤ 50 mM, the mixed micelles are globular interacting micelles. Furthermore the micelle aggregation number reflects the aggregation numbers of the pure component micelles as observed in the ternary mixtures. The addition of R1 and R2 has little impact on the micelle aggregation number (see table 4). Typically the aggregation number of R1 and R2 are ~ 35-45 in this concentration range, similar to that for LAS (43) and their corresponding pp values are ≥ 0.5 (24). The molecular constraints associated with R1 and R2 have some impact upon molecular packing and hence the values of r_1, r_2 and ee; as the fully extended alkyl chain length associated with the the di-C_{10} of R1 and R2 is ~14 Å and the headgroup volumes are similar to that for $C_{12}E_8$. R2 with its larger di-rhamnose headgroup is fairly globular in this concentration range, whereas R1 has a greater tendency towards planar structures for concentrations ≥ 30 mM. A notable feature of the self-assembly of R1 and R2 and their mixtures is the relatively low degree of ionisation, which varies from ~ 0.1 for R2 to ≤ 0.2 for R1 rich compositions of R1 / R2 mixtures. It was observed in the study of the self-assembly and surface adsorption of R1 and R2 that they are are only weakly ionic, and behave more like nonionic surfactants (24, 25). Hence a feature of the mixed micelles of $C_{12}E_8$ / LAS / SLES is that the low degree of ionisation is even lower when part of the $C_{12}E_8$ / LAS / SLES is replaced by R1 / R2. δ is then typically ~ 0.15, due to the effective increase in the nonionic components in the mixed micelle with the addition of R1

and R2. However, the most striking feature of the 5-component mixture is that for LAS rich compositions of the $C_{12}E_8$ / LAS / SLES ternary mixture, the addition of R1 / R2 results in a transition towards planar lamellar / vesicular structures. Depending upon the relative amounts of LAS, R1 and R2, and the R1 / R2 composition the solution microstructure is in the from of either L_1 / L_α or L_α / L_1 coexistance. The tendency towards the more planar structures is greater at higher surfactant concentrations, greater LAS mole fractions, and greater R1 / R2 and R1 mole fractions. At the concentrations studied the transition is not observed in the binary or ternary mixtures involving $C_{12}E_8$, LAS, and SLES, nor in the R1, R2 and R1 / R2 solutions at concentrations realtive to those in the 5-component mixtures. However it is know that LAS and R1 have a tendency towards the formation of planar structures, and which is most pronounced at higher concentrations (24, 25, 43, 45). The observations of the onset of the formation of planar structures in the 5-component mixtures imply that there is a synergistic packing which enhances the onset towards the planar structures associated with R1 and LAS. It occurs only for the LAS rich compositions $C_{12}E_8$ / LAS / SLES and is enhanced as the amount of R1 present increases. This is in part due to the favourable pp associated with R1 and LAS. In ionic surfactants the occurrence of more planar structures is usually associated with higher surfactant concentrations, and this is attributed to an increased electrostatic screening as the concentration increases, which helps to reduce the area/molecule, A, and increase the pp value. As $C_{12}E_8$ is nonionic, and SLES, R1 and R2 are only weakly ionic, the combination of R1 / R2 / $C_{12}E_8$ / LAS / SLES is effective in increasing the intra-micellar electrostatic repulsion, and so promote more effective headgroup packing.

CONCLUSIONS

Understanding the nature of self-assembly is important in the context of the formulation and performance of many home and personal care products. How biosurfactants interact with conventional surfactants will have a great bearing on how they can be incorporated effectively into such formulations. The SANS results presented here substantially extend the exploration pof self-assembly in dilute multi-component surfactant mixtures (41-43), and the role of biosurfactants in surfactant mixing (23-27). The SANS data show that the mixtures of $C_{12}E_8$, LAS, and SLES, a ternary mixture which is the basis og many current formulations, are consistent with globular interacting micelles with sizes and aggregation numbers that reflect a solution composition weighted average of the pure component micelles. The relatively low degree of ionisation of the micelles is consistent with the presence of the $C_{12}E_8$ nonionic

surfactant and the weakly ionic nature of SLES. Upon the addition of the rhamnolipids R1 and R2 there is a transition towards planar structures when the solutions compositions are relatively rich in LAS. This is not observed in the binary and ternary mixtures of $C_{12}E_8$, LAS, and SLES or in the R1 / R2 mixtures at the relatively low concentrations studied here (24, 25). Such a transition is not widely observed, and provides an insight into the packing associated with multi-component surfactant mixtures, and the potential to manipulate the preferred curvature in such mixtures. At compositions less rich in LAS, the addition of the rhamnolipids has little impact, and globular micellar structures are retained. The results illustrate that synergistic packing effects occur and can be used to tailor or manipulate microstructure; and this is a potentailly riuch area for future investigations. The weakly ionic nature of the 5-component mixed micelles implies that the solutions will be relatively insensitive to the addition of electrolyte, and exhibit a high degree of tolerance to hard water; and future SANS measurements and complementary studies will be required to persue this hypothesis.

ACKNOWLEDGEMENTS

The provision of beam time at ISIS and the ILL, and the invaluable help, expertise and technical support of the facility staff is acknowledged.

SUPPORTING INFORMATION

Some additional SANS results, in the form of tables and plots, are included in the Supporting Information.

AUTHOR INFORMATION

Corresponding author: jeff.penfold@stfc.ac.uk

Author Contributions: All the authors have given their approval of the final version of the manuscript.

Funding Sources: Funded through an EPSRC CASE award with Unilever R and D, and neutron beam time provided by the ISIS and ILL facilities.

REFERENCES

(1) Ron, E, Z; Rosenberg, E. Natural role of biosurfactants: mini review, Environ. Microbiol. 2001, 2, 229-236

(2) Muthosamy, K; Gopalakrishan, S; Kockupappy, T; Sivachidamboram, P, Biosurfactants: properties, commercial production and applications, Curr. Sci. 2008, 95, 736-747

(3) Desai, J. D; Banat, I. M, Microbial production of surfactants and their commercial potential, Mol. Biol. Rev. 1997, 61, 47-64

(4) Banat, I. M; Mukhar, R. S; Cameota, S. S; Potential commercial applications of microbial surfactants, Appl. Microbiol. Biotechnol. 2000, 53, 495-508

(5) Singh, P; Cameotra, S. S, Potential applications of microbial surfactants in biomedical sciences, Trends Biotechnol. 2004, 22, 142-146

(6) Milligan, C. N, Environmental applications of biosurfactants, Environ. Pollut. 2005, 113, 183-198

(7) Georgiou, G; Lu, S. S; Sharma, M. M; Surface active components from micro-organisms, Biotechnology, 1992, 10, 60-65

(8) Kitamoto, D; Morita, T; Fukuota, T; Konishi, M; Imura, T, Self-assembly properties of glycolipid biosurfactants and their potential applications, Curr. Opin. Coll. Int. Sci. 2009, 14, 315-328

(9) Nitschke, M; O'Costa, S.G.V.A; Contiero, J, Rhamnolipid surfactants: an update on the general aspects of these remarkable biomolecules, Biotechnol. Prog. 2005, 21, 1593-1600

(10) Batghi, M, K; Fazaelipoor, M. H. Application of rhamnolipid in the formulation of a detergent, J. Surfact. Deterg. 2012, 15, 679-684

(11) Randhawa, K. K. S; Rahman, P. K. S. M. Rhamnolipid biosurfactants: past present and future scenario of global market, Frontiers in Microbiology, 2014, 5, 1-7

(12) Perfumo, A; Rudden, M; Smyth, T. J. P; Marchant, R; Stevenson, P. S; Parry, N. J; Banat, I. M, Rhamnolipids are conserved biosurfactant molecules: implications for their biotechnological potential, Appl. Microbiol. Biotechnol. 2013, 97, 7297-7306

(13) Abolas, A; Pinazo, A; Infante, M. R; Casals, M; Garcia, F; Manresa, A, Physicochemical and anti-microbial properties of new rhamnolipids produced by Pseudomonas aeruginosa AT10 from soybean refinery wastes, Langmuir, 2001, 17, 1367-1371

(14) Helvaci, S. S; Peker, S; Ozdemir, G; Effects of electrolytes on the surface properties of rhamnolipids R1 and R2, Coll. Surf. B, 2004, 35, 225-233

(15) Peker, S; Helvaci, S. S; Ozdemir, G, Interface-subphase interactions in aqueous rhamnose solutions, Langmuir, 2003, 19, 5838-5845

(16) Zhong, H; Zeng, G. M; Liu, J. X; Xu, X. M; Yuan, X. Y; Fu, H. Y; Huang, G. H; Liu, Z; Ding, Y, Adsorption of monorhamnolipid and dirhamnolipid of two Pseudomonas aeruginosa strains and the effect of cell hydrophobicity, Appl. Microbiol. Biotechnol. 2008, 79, 671-677

(17) Ozdemir, G; Peker, S; Helvaci, S. S, Effect of pH on the surface and interfacial behaviour of rhamnolipids R1 and R2, Coll. Surf. A, 2004, 234, 135-143

(18) Guo, Y. P; Hu, Y. Y; Ciu, R. R; Lu, H, Characterisation and micellisation of rhamnolipidic fractions and crude extracts produced by Pseudomonas aeruginosa mutant MIG-N146, J. Coll. Int. Sci. 2009, 331, 356-363

(19) Wang, H; Cross, C. S; Mudalige, A; Polt, R. L; Pemberton, J. E. A PM-IRRAS investigation of monorhamnolipid orientation at the air-water interface, Langmuir, 2103, 29, 4441-4450

(20) Sanchez, M; Aranda, K. J; Espuny, M. J; Marques, A; Terval, J. A; Manresa, A; Ortz, A; Aggregation behaviour in a dirhamnolipid biosurfactant secreted by Pseudomonas aeruginosa in aqueous media, J. Coll. Int. Sci. 2007, 207, 246-253

(21) Dahranzma, B; Milligan, C. N; Nieh, N. P; Effects of additives on the structure of rhamnolipid (biosurfactant): a small angle neutron scattering study, J. Coll. Int. Sci. 2008, 319, 590-593

(22) Pornsunthorntawee, O; Chavadej, S; Rujiravanit, R; Solution properties and vesicle formation of rhamnolipid biosurfactants produced by Pseudomonas aeruginosa SP4, Coll. Surf. B, 2009, 72, 6-15

(23) Manko, D; Zdziennicka, A; Janezuk, B; Thermodynamic properties of rhamnolipid micellisation and adsorption, Coll. Surf. B, 2014, 119, 22-29

(24) Chen, M. L; Penfold, J; Thomas, R. K; Smyth, T. J. P; Perfumo, A; Marchant, R; Banat, I. M; Stevenson, P; Parry, A; Tucker, I; Grillo, I, Solution self-assembly and adsorption at the air-water interface of the monorhamnose and dirhamnose rhamnolipids and their mixtures, Langmuir, 2010, 26, 18281-18292

(25) Chen, M. L; Penfold, J; Thomas, R. K; Smyth, T. J. P; Perfumo, A; Marchant, R; Banat, I. M; Stevenson, P; Parry, A; Tucker, I; Grillo, Mixing behaviour of the biosurfactant rhamnolipid with a conventional anionic surfactant, sodium dodecyl benzene sulfonate, Langmuir, 2010, 26, 17958-17968

(26) Song, D; Li, Y; Liang, S; Wang, J, Micelle behaviours of sophorolipid / rhamnolipid binary mixed surfactant systems, Coll. Surf. A, 2013, 436, 201-206

(27) Haba, E; Pinazo, A; Pons, R; Perez, L; Manresa, A, Complex rhamnolipid mixture characterisation and its influence on DPPC bilayer organisation, Biochimica et Biophysica Acta, 2014, 1838, 776-783

(28) Mixed Surfactant Systems, Eds M Abe, J F Scamehorn, Marcel Dekker, NY, Surfactant Science Series, Vol 124, 2005

(29) Holland, P. M. Non-ideal mixed micellar solutions, Adv. Coll. Int. Sci. 1986, 26, 111-129

(30) Holland, P. M; Rubingh, D. N; Non-ideal multi-component mixed micelle model, J. Phys. Chem. 1983, 87, 1984-1990

(31) Holland, P. M, Non-ideality at the interface in mixed micellar systems, Coll. Surf. 1986, 19, 171-183

(32) Shiloach, A; Blankschtein, D, Predicting micellar properties of binary surfactant mixtures, Langmuir, 1998, 14, 1618-1631

(33) Kamrath, R. F; Franses, E. I. Mass-action model in mixed micellisation, J, Phys. Chem. 1984, 88, 1642-1648

(34) Lu, J. R; Thomas, R. K; Penfold, J, Surfactant layers at the air-water interface: structure and composition, Adv. Coll. Int. Sci. 2000, 84, 143-304

(35) Penfold, J; Thomas, R. K, Mixed surfactant at the air-water interface, Annu. Rep. Prog. Chem. Sect C, 2010, 106, 14-35

(36) Penfold, J; Thomas, R. K, The limitations of models of surfactant mixing at interfaces, as revealed by neutron scattering, PCCP, 2013, 15, 7017-7027

(37) Hines, J. D; Thomas, R. K; Garrett, P. R; Rennie, G. K; Penfold, J, A study of the interactions in a ternary surfactant systems in micelles and adsorbed layers, J. Phys. Chem. B, 1998, 102, 9708-9713

(38) Staples, E; Thompson, L; Tucker, I; Penfold, J, Effect of dodecanol on mixed non-ionic and non-ionic / anionic adsorption at the air-water interface, Langmuir, 1994, 10, 4136-4141

(39) Liley, J; Penfold, J; Thomas, R. K; Tucker, I; Petkov, J. T; Stevenson, P; Webster, J. R. P, Surface adsorption in ternary surfactant mixtures, to be published

(40) Liley, J; Penfold, J; Thomas, R. K; Tucker, I; Petkov, J. T; Stevenson, P; Banat, I; Marchant, R; Rudden, M; Webster, J. R. P, Adsorption at the air-water interface in biosurfactant-surfactant mixtures, to be published

(41) Penfold, J; Staples, E; Thompson, L; Tucker, I; Hines, J; Thomas, R. K; Lu, J. R; Warren, N, The structure and composition of mixed surfactant micelles of SDS / $C_{12}E_6$ and $C_{12}E_6$ / C_{16}TAB, J. Phys. Chem. B 1999, 103, 5204-5211

(42) Penfold, J; Tucker, I; Thomas, R. K; Staples, E; Schuermann, R, Structure of mixed anionic / non-ionic surfactant micelles: experimental observations relating to the role of the headgroup electrostatic and steric effects and the effects of added electrolyte, J. Phys. Chem. B, 2005, 109, 10760-10770

(43) Penfold, J; Thomas, R. K; Dong, C. C; Tucker, I; Metcalfe, K; Golding, S; Grillo, I, Equilibrium surface adsorption behaviour in complex anionic / non-ionic surfactant mixtures, Langmuir, 2007, 23, 10140-10149

(44) Petkov, J. T; Tucker, I; Penfold, J; Thomas, R. K; Petsev, D. N; Dong, C. C; Golding, S; Grillo, I, The impact of multivalent counterions Al^{3+} on the surfactant adsorption and self-assembly of anionic surfactant alkyloxyethylene sulphate and anionic / non-ionic surfactant mixtures, Langmuir, 2010, 26, 16669-16709

(45) Ma, J. G; Boyd, B. J; Drummond, C. J, Positional isomers of linear sodium dodecyl benzene sulfonate, solubility, self-assembly and air-water interfacial activity, Langmuir, 2006, 22, 8646-8654

(46) Hayter, J. B; Penfold, J; Determination of micelle structure and charge by small angle neutron scattering, Colloid Polym. Sci. 1983, 261, 1022-1030

(47) Hayter, J. B; Penfold, J; An analytic structure factor for macroion solutions, Mol. Phys. 1981, 42, 109-118

(48) Hayter, J. B; Hansen, J. P, A rescaled MSA structure factor for dilute charged colloidal dispersions, Mol. Phys. 1982, 46, 651-656

(49) Heenan, R, K; Penfold, J; King, S. M, SANS at pulsed neutron sources: present and future prospects, J. Appl. Cryst. 1997, 30, 1140-1147

(50) Heenan, R. K; King, S. M; Turner, D. S; Treadgold, J. R, SANS2D at the ISIS 2nd Target station, Proc. ICANS XVII, 2006, 780-785

(51) Dewhurst, C. D, D33, a third small angle neutron scattering instrument at the ILL, Meas. Sci. Technol. 2008, 19, 034007-034011

(52) Ghosh, R. E; Egelhaaf, S. U; Rennie, A, ILL Internal Report, 1989, ILL98GH14T

(53) Heenan, R. K; King, S. M; Osborn, R; Stanley, H. B. RAL Internal Report, 1989, RAL-89,128

(54) Xu, H; Penfold, J; Thomas, R. K; Petkov, J. T; Tucker, I; Grillo, I; Terry, A, Impact of Al^{3+} on the self-assembly of the anionic surfactant sodium polyethylene glycol monoalkyl ether sulphate in aqueous solution, Langmuir, 29, 2013, 13359-13366

(55) Xu, H; Ma, K; Li, P. X; Thomas, R. K; Penfold, J; Lu, J. R. Limitations in the application of the Gibbs equation to anionic surfactants at the air-water interface: SDS and SLES above and below the cmc, Langmuir, 2013, 29, 9335-9351

(56) J N Israelachvili, D J Mitchell, B W Ninham, Theory of self-assembly of hydrocarbon amphiphiles into micelles and bilayers, J. Chem. Soc. Faraday Trans. 2, 1976, 72, 1525-1568

(57) E Caponetti, R Triolo, O C Ho, J S Johnson, L J Magid, P Butler, K A Payne, A small angle neutron scattering (SANS) study of micellar structure and growth of a straight chain benzene sulfonate: comparison with an isomeric branched chain surfactant, J. Coll. Int. Sci. 1987, 116, 200-210

(58) J B Hayter, A self-consistent theory of dressed micelles, Langmuir, 1992, 8, 2873-2876

GRAPHICAL ABSTRACT

Self-assembly in dilute mixtures of non-ionic, and anionic surfactants and rhamnolipid biosurfactants

J. Liley, J. Penfold, R. K. Thomas, I. M. Tucker, J. T. Petkov, P. S. Stevenson, I. M. Banat, R. Marchant, M. Rudden, A. Terry, I. Grillo

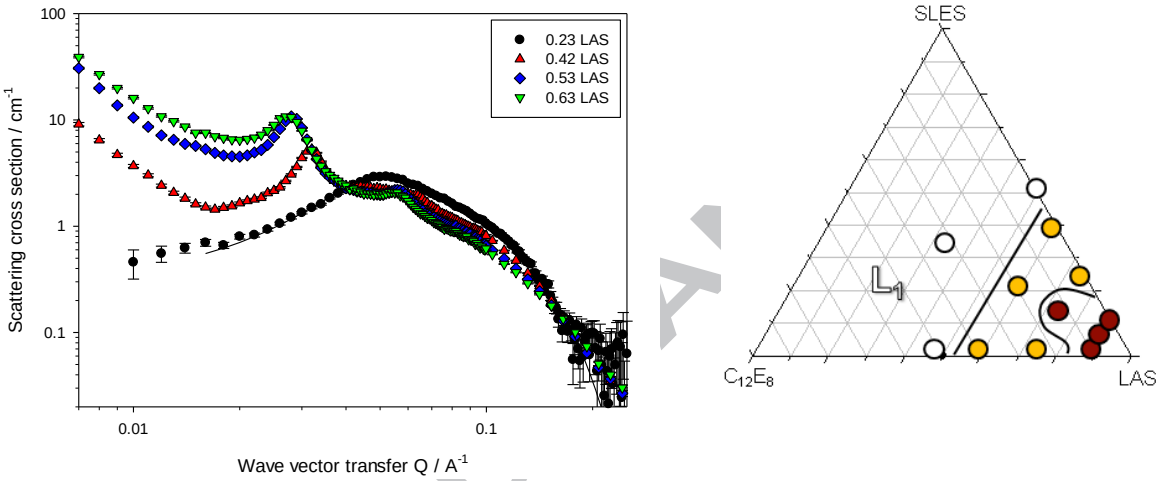

Keywords: mixed surfactants; biosurfactants; slef-assembly; mixed micelles; small angle neutron scattering